



## **1. Introduction**

Stress corrosion cracking (SCC) is a mechanical–environmental failure process in which sustained tensile stress well below the yield stress of the material and chemical attack combine to initiate and propagate fracture in metallic parts. SCC is often difficult to detect prior to component fracture, since the failure takes the form of fine cracks that penetrate deep into the component with little or no evidence of corrosion on the external surface. In failures involving SCC, the crack initiation and propagation may respond in different ways in different environments. While the crack initiation depends on the bulk environment, the crack propagation depends on the crack-tip environment and the microstructural constituents in the material. Generally, SCC takes place by extensive branching and proceeds in a direction perpendicular to the direction of stresses contributing to their initiation and propagation [1]. Crack initiation occurs due to localized electrochemical dissolution of the metal. The protective films that form at the crack tip get ruptured with sustained tensile stresses, resulting in exposure of fresh anodic metal to the corrosive medium continuously and hence, the SCC propagates progressively over a period of time.

Bellows expansion joints manufactured from austenitic stainless steels are extensively used for various applications in space and nuclear industries and these joints are often exposed to liquid fuel and propellant [2–6]. Other applications of

bellows include heating systems of steam and water in petrochemical industries. Under the application environment, the bellows are subjected to both mechanical stresses and corrosion environment, and hence, are prone to failures due to progressive damage. Fatigue, corrosion fatigue, and SCC are common mechanisms of failures of bellows manufactured from austenitic grade stainless steels [2–4]. The present paper discusses recurring failure of bellows made of AISI 316L grade stainless steel. The bellows, manufactured from a double ply sheet of thickness 0.2 mm, was installed in a pressure safety valve (PSV) of a hydrocracker unit in a petroleum refinery plant.

## 2. The failure

There was a series of failure of bellows installed in a PSV of a hydrocracker unit leading to leakage of process fluid. The first failure of the bellows took place after 13 years of service. After the first failure, the bellows was replaced by a new one. However, the failure continued to occur and in total, there were three consecutive failures in a span of one week duration. On-site inspection showed several cracks on the outer surface of the bellows. The operating pressure and temperature of the PSV were  $1.6 \text{ kg/cm}^2$  and  $100^\circ\text{C}$  respectively. The construction of the PSV is illustrated schematically in Fig. 1.

## 3. Laboratory investigation

### 3.1. Macroscopic examination

Fig. 2(a) shows the photograph of one of the cracked bellows. On observation under stereo-binocular microscope, several cracks were detected on the external surface of the bellows (Fig. 2(b)). The cracks were located on the convolution crest and were oriented along the bellows axis. There were no cracks at the convolution root regions.

A suitable cut was made in the bellows and the two plies of the bellows were separated out. Examination showed presence of cracks in the inner ply as well. In this case, the cracks were also located at the convolution crest and not at the convolution root. The population of cracks in the inner ply was, however, several times less than that in the outer ply.

The bellows used in the PSV was of 'S'-type and the construction is shown schematically in Fig. 3. The orientation of the cracks on the convolution crest is also shown. In the as-received condition, the bellows surface was found to be clean and shiny in appearance. There were no external deposition or corrosion products on the surface. However, the bellows was cleaned prior to dispatch to the laboratory for investigation.

### 3.2. Mode of crack propagation

A few cracks were pulled open for scanning electron fractographic study. Fig. 4(a) shows an opened surface of one of the cracks on the outer ply of the bellows. It can be seen that the cracking of the bellows had occurred by intergranular mode of

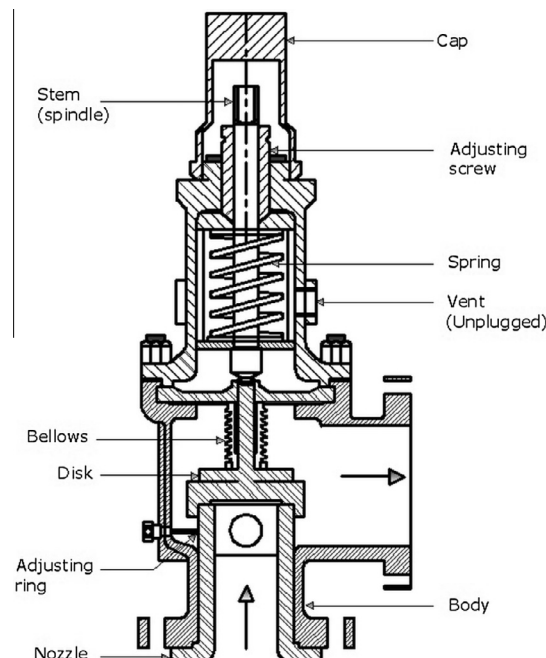
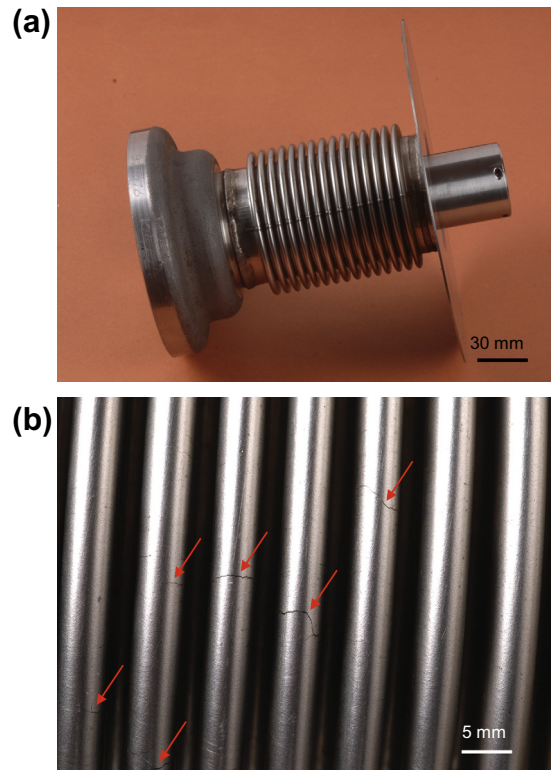
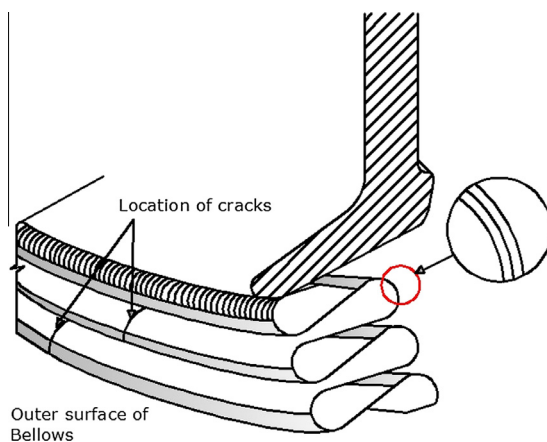


Fig. 1. Schematic showing the bellows in the pressure safety valve (PSV) assembly.



**Fig. 2.** (a) Failed bellows, and (b) close-up view showing cracks (arrows) on the convolution crest regions.



**Fig. 3.** Schematic diagram showing construction of the bellows and the location of cracks on the bellows surface.

crack propagation (**Fig. 4(b)**). The crack surface also showed presence of a number of secondary cracks in a direction perpendicular to the main crack surface.

### 3.3. Compositional analysis on crack surfaces

Several locations on the crack surfaces were covered with firmly adherent corrosion products (**Fig. 5**). In-situ compositional analysis performed by energy dispersive X-ray (EDX) analyzer showed that the corrosion products contained chlorine and oxygen in significant concentrations in addition to the elements of the base material (**Fig. 6, Table 1**). The concentration of chlorine in the corrosion products was determined to be as high as 6 wt%.

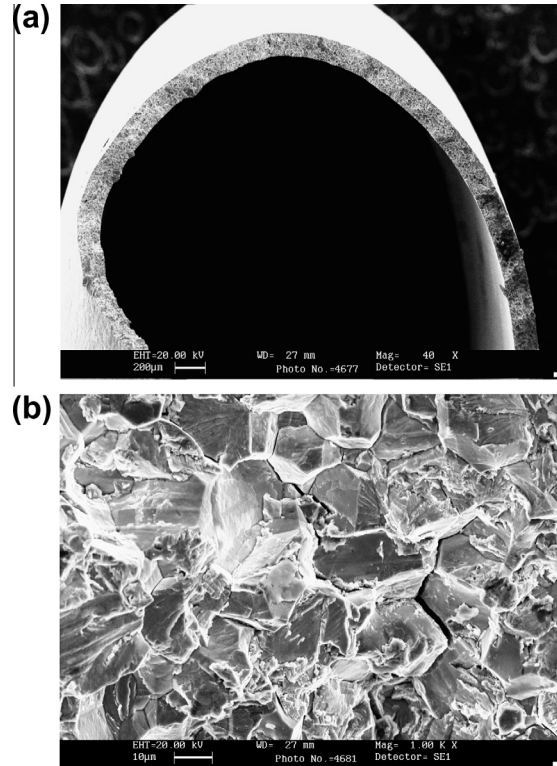


**Fig. 4.** (a) Secondary electron image of a crack surface, and (b) intergranular mode of crack propagation with secondary cracks at the grain boundaries.

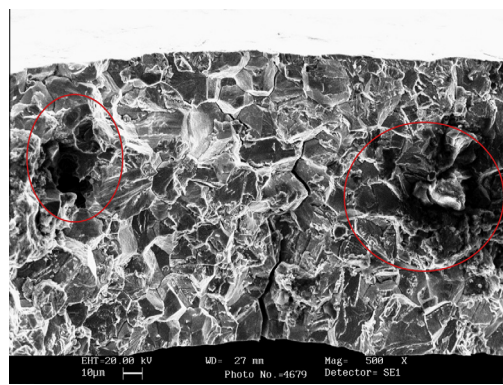


**Fig. 5.** Secondary electron fractograph showing presence of firmly adherent corrosion products on the crack surface (encircled).

### 3.4. Metallographic examination

A few samples containing cracks were cut from the plies of the bellows, mounted on the cross section along the transverse direction of the bellows and metallographically prepared. Fig. 7 shows the cross section of the plies of the bellows in an unetched condition. A few through and propagating cracks in the outer ply of the bellows can be seen. Fig. 8(a) shows a typical propagating branching crack initiating from the outer surface of the bellows. The origins of crack initiation were corrosion pits on the outer surface. The magnified view of the cracked region is shown in Fig. 8(b). Although the branching cracks are predominantly intergranular in nature, transgranular crack propagation can be seen at a few locations (Fig. 8(b)).

Fig. 9(a) shows a secondary electron image of the cross section of the inner ply in the vicinity of a through crack in the outer ply. Magnified view of the region is shown in Fig. 9(b). Initiation of a number of cracks on the outer surface of the inner ply can be seen. At a few places, the cracks were found to have propagated through the thickness of both the plies of the bellows (Fig. 10).

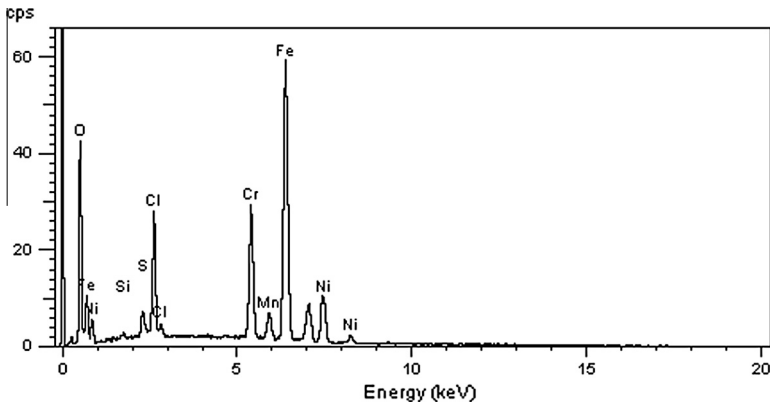


**Fig. 6.** Energy dispersive X-ray spectrum of corrosion products on the fracture surface shown in Fig. 5.

**Table 1**

Semi-quantitative compositional analysis of the bellows material and the corrosion products; carried out by energy dispersive X-ray (EDX) analysis.

Element	Composition (wt%)									
	C	O	Si	S	Cl	Cr	Mn	Mo	Ni	Fe
316L Specification	0.03	–	0.75	–	–	16.0–18.0	2.0	2.0–3.0	10.0–14.0	Balance
Bellows material	– <sup>a</sup>	–	0.6	–	–	17.8	1.7	2.4	11.0	Balance
Corrosion products on the fracture surface	– <sup>a</sup>	23.6	0.2	0.7	5.9	12.7	1.4	–	11.7	Balance

<sup>a</sup> Carbon cannot be determined accurately by EDX analysis.

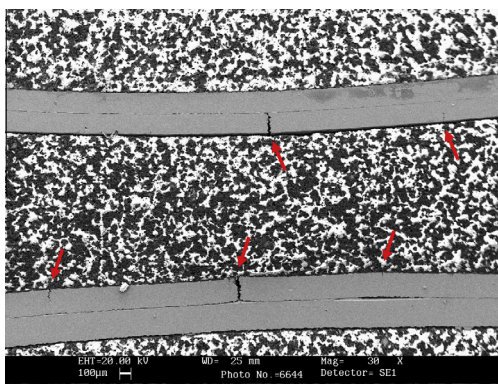


**Fig. 7.** Secondary electron micrographs of two transverse sections of the bellows showing through cracks (arrows) in the outer ply.

### 3.5. Analysis of bellows material

Compositional analysis showed that the bellows was made of 316L grade austenitic stainless steel and it conformed to the design specification (Table 1). The optical microstructures of the bellows material are shown in Fig. 11. It consisted of austenite grains. There was no predominance of carbide precipitation at the grain boundaries, eliminating the possibility of sensitization of steel. Microstructural examination, however, revealed extensive formation of shear bands and deformation twins within the austenite grains (Fig. 11(a)). Also, at the central region of the sheet cross section, the microstructure showed presence of stress induced martensite phase (Fig. 11(b)).

Hardness of the bellows material was determined on longitudinal section of the bellows using Vickers micro-hardness tester at a load of 100 g. The hardness values were found to be in the range 215–302 HV, confirming that the bellows was fabricated from cold rolled austenitic stainless steel sheet. Results of the hardness survey, however, showed that average hardness at the convolution crest was significantly higher than that at the convolution root as well as other locations of both the plies of the bellows (Fig. 12).

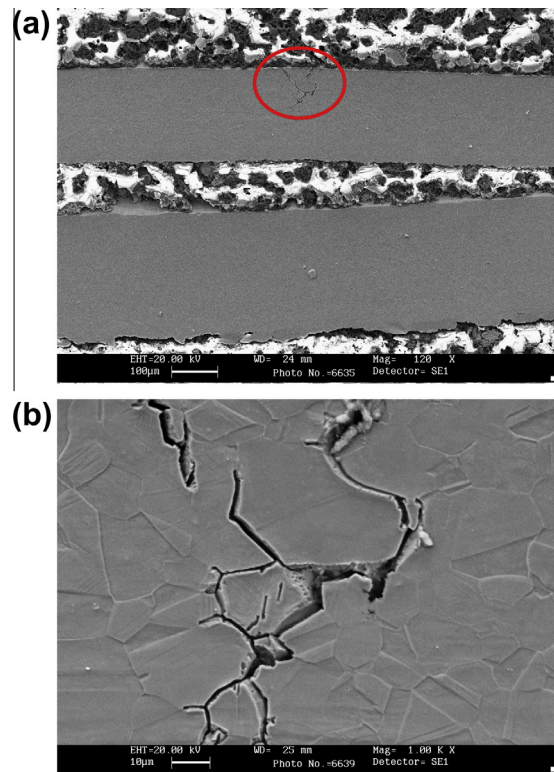


**Fig. 8.** Secondary electron micrographs (etched with aqua regia) showing (a) crack initiation region (encircled) on the outer ply of the bellows, and (b) magnified view showing branching cracks.

#### 4. Discussion

Laboratory investigation showed that all three bellows failures in the PSV of the hydrocracker unit were identical in nature. There was severe cracking in both inner and outer plies of the bellows leading to leakage of the process fluid.

##### 4.1. Failure mechanism

Fractographic and metallographic studies showed that the cracks in the plies of the bellows have propagated predominantly by intergranular mode, and they were branching in nature. In several places, the crack surfaces were covered with firmly adherent corrosion products. In-situ compositional analysis showed that the corrosion products contained chlorine in concentrations as high as 6 wt%. The branching cracks in the bellows and presence of corrosion products on the fracture surface are characteristic of SCC. High concentration of chlorine in the corrosion products also indicates that the failure of the bellows was by chloride SCC.

Laboratory investigation confirmed that the stress corrosion cracks had initiated on the outer surface of the bellows. It is, therefore, apparent that the source of chloride ions was the environment surrounding the outer surface of the bellows. Once there were through cracks in the outer ply of the bellows, the inner ply was exposed to corroding media. It has been shown that the cracks in the inner ply had also initiated on the outer surface. When both the plies of the bellows developed through cracks, there was leakage of process fluid from the PSV.

##### 4.2. Micro-mechanism of crack propagation

Chloride SCC in austenitic stainless steel usually occurs in the temperature range 60–200 °C [1]. In the present case, the process fluid temperature is 100 °C and hence, if chloride ions are present in the environment in sufficient concentration, chloride SCC in the bellows is likely to occur.

It is well known that in the presence of chloride ions, SCC in austenitic stainless steels proceeds in transgranular mode [1]. Scanning electron fractographic study, however, showed that in the case of present failure, the micro-mechanism of crack propagation was predominantly by intergranular mode. Although this is unusual, intergranular chloride SCC has been reported to occur in 316L stainless steel under certain conditions. For example, during chloride SCC of austenitic stainless steel, crack propagation takes place by intergranular mode if the grain boundaries are anodic with respect to the grain bodies

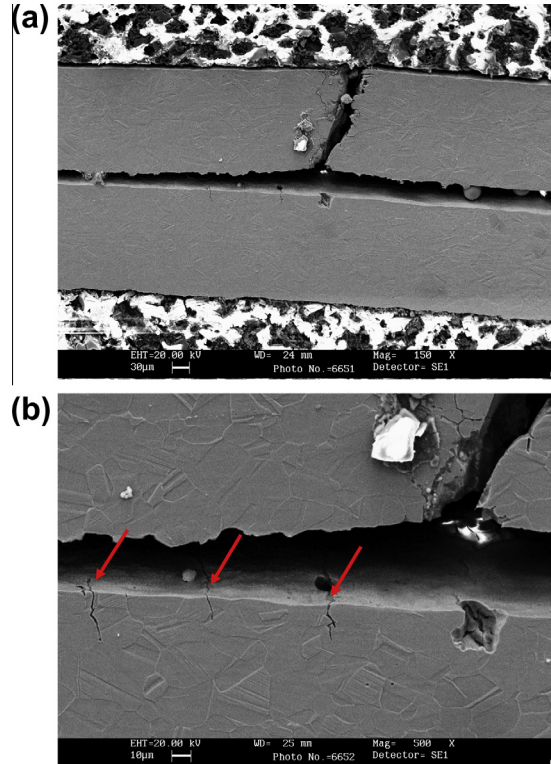


**Fig. 9.** Secondary electron micrographs showing (a) a through crack in the outer ply of the bellows, and (b) cracks in the inner ply in the vicinity of the through crack in outer ply shown in (a).

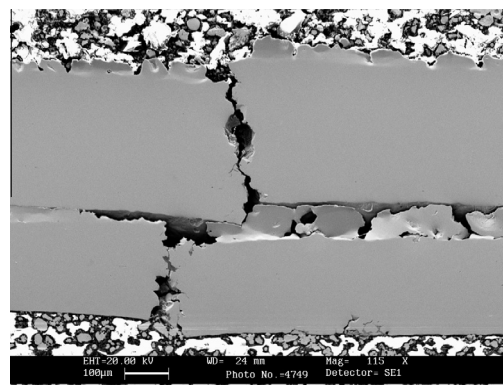


**Fig. 10.** Secondary electron micrograph showing through thickness crack in both the plies of the bellows.

[1,7,8]. This is commonly the case, when the material is sensitized. In sensitized steel, the precipitation of chromium carbide at the grain boundaries results in chromium depleted zones adjacent to the grain boundaries. The chromium depleted zones along the grain boundaries are anodic to the main body of the grains, and hence, SCC progresses intergranular [7,8]. Microstructural study of the bellows material, however, did not show grain boundary carbide precipitation. Hence, inference can be drawn that the intergranular mode of crack propagation in the present case is because of reasons other than sensitization of steel.

In spite of the microstructure being not sensitized, intergranular mode of SCC can still occur in austenitic grades of stainless steel under certain specific conditions. Intergranular SCC in austenitic stainless steels has been reported [1] in boiling-water nuclear reactors where the steels were free from grain-boundary carbides but they were used in heavily cold-worked condition. It is well known [9–11] that in 316L stainless steels, the austenite phase is not absolutely stable under stress. Plastic deformation can induce transformation of austenite to martensite phase. Presence of deformation induced martensite phase in the microstructure facilitates intergranular crack propagation during SCC in the following two ways:

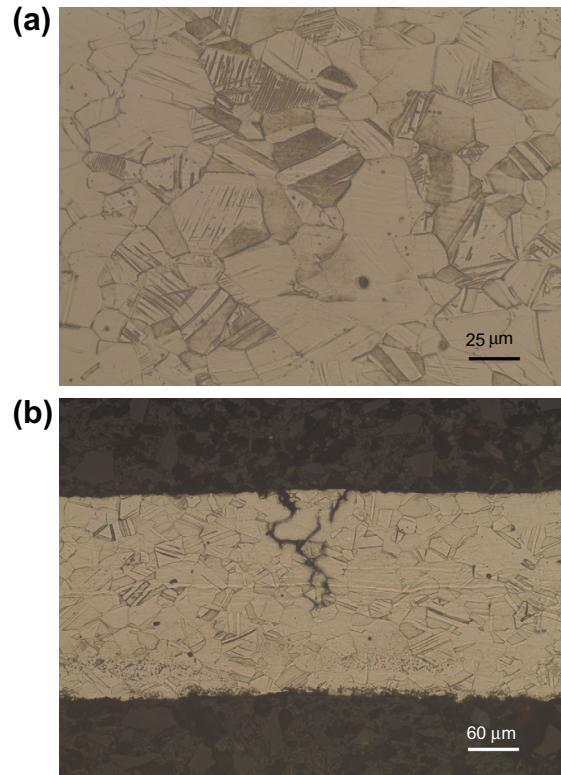


**Fig. 11.** Optical micrographs (etched with aqua regia) showing (a) shear bands and twins within the austenite grains, and (b) stringers of stress induced martensite phase at the mid-section of the sheet.

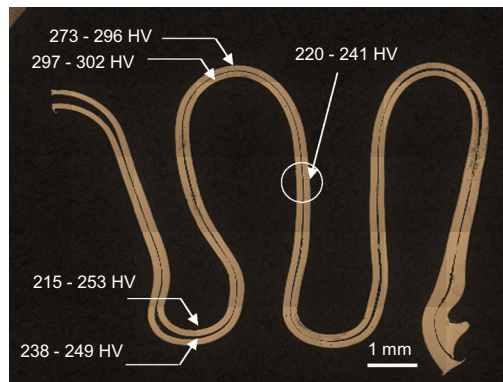


**Fig. 12.** A montage of optical micrographs of the longitudinal section of a part of the bellows; note significantly higher hardness at the convolution crest relative to that at the convolution root.

- (a) Dissolution rate of martensite in corrosive environment is much higher than austenite, and hence, crack propagation occurs preferentially along the martensite phase [10].
- (b) Martensite phase has high hydrogen diffusivity and low hydrogen solubility in comparison to austenite phase. Hence, presence of martensite phase in the microstructure induces hydrogen embrittlement and thereby, the crack propagation can occur by intergranular mode. The source of hydrogen is the in-situ generation of nascent hydrogen by electrochemical reaction that takes place during SCC [9].

In general, cold worked sheet materials are used for fabrication of bellows. This is necessary to impart structural stiffness to the component. Cold working often introduces shear bands within the austenitic grains in concurrence with stress induced martensitic transformation in the material. Metallographic study confirmed that the sheet material used in the con-

struction of the bellows was in a cold worked condition and the microstructure contained shear bands as well as stress induced martensite phase. Hence, intergranular mode of crack propagation during chloride SCC in the present case is justifiable.

#### 4.3. Crack initiation at the convolution crest of the bellows

It has been established through fractographic and metallographic studies that all cracks have initiated at the convolution crest. In none of the failed bellows studied, did crack initiation occur at the convolution root irrespective of whether they are in outer or inner ply of the bellows.

Sitko and Skoczen [12] carried out finite element modeling studies on strain induced martensite formation in austenite grade stainless steel such as 316L in different structural members. It has been shown that the propensity of strain induced martensite formation in the bellows is more at the bent regions, namely, convolution crest and root.

Bellows expansion joints used in structural assemblies are subjected to thermal as well as mechanical stresses. The load-deflection characteristics are taken into consideration while designing the specific geometry of the bellows depending on the application [13]. In addition to satisfying the criterion for mechanical stresses, the corrosion resistance of the material to application corrosion environment was taken into account. Austenitic grade stainless steels meet these requirements and hence, are extensively used for applications such as nuclear power plants and petrochemical industries. Depending on the application, several categories of bellows such as universal, gimbal and hinged, are used. Similarly, varieties of convolution shapes such as 'S', 'U' 'Ω' are used depending on the requirement and cost of manufacture [14]. In the present case, the bellows used was of the 'S' type.

Bellows are manufactured from thin walled tubular section using roll forming or hydro-forming techniques. These methods of manufacture impart differential cold work at different regions of the bellows such as the convolution crest and the root. As a result, the strength of the material is locally changed and the resistance of the material to cyclic loading as well as corrosion attack varies with location on the bellows surface. It has been reported [15] that with regard to fatigue, a combination of roll and hydro-forming is a better proposition for fabrication of bellows. In the same study, it has also been established that in hydro-formed bellows of austenitic grade stainless steels, the crest regions undergo more cold work compared to the root. The results of the hardness survey (**Table 2**) conducted on the failed bellows also suggest a similar variation in cold work. Higher the amount of cold work, higher is the volume fraction of deformation induced martensite phase in the material. Hence, the initiation of cracks preferentially at the convolution crests is explainable.

#### 4.4. Source of chloride ions

The pipeline on which the PSV was installed carried hydrocarbon as the process fluid. This hydrocarbon was an unlikely source of chloride ions because (i) it was at the final stage of refining for the production of motor spirit, and (ii) its quality was being monitored regularly. Also, considering initiation of SCC on the outer surface of the bellows, it is apparent that the environment around the bellows was contaminated with chloride ions and not the hydrocarbon.

It is significant to note that the first failure of the bellows occurred after about 13 years of service of the PSV. Subsequently, there were two more failures of similar nature in the same PSV in a span of one week. Three consecutive failures in such a short time are unexplainable unless there was a source of chloride ions in the system itself, which might have originated shortly before the first failure took place. Hence, the process and the operational history of the hydrocracker unit were examined in detail for identifying the probable source(s) of the chloride ions.

**Fig. 13** shows the process flow chart and associated equipment in the vicinity of the failed PSV. The PSV is mounted on the feed coalescer which discharges feedstock to the recycle splitter column. In another line and prior to the recycle splitter column, there is a system for removal of heavy polynuclear aromatics (HPNA) from the feedstock. The HPNA system consists of two beds filled with activated carbon. The HPNAs are adsorbed onto the activated carbon for increasing the downstream hydrocracker catalyst life and avoiding HPNA fouling of feed effluent heat exchangers. The outlet of the HPNA system also joins the splitter column. The outlet pipelines of the HPNA system and the PSV are interconnected. The pressures of both the systems, that is, feed coalescer discharge and the HPNA system are equal.

The HPNA bed contains granulated activated carbon which is supported by stainless steel screen. It was discovered that there was a failure in the HPNA bed prior to the first failure of the bellows. The failure was in the stainless steel screen. Laboratory tests revealed that this particular batch of activated carbon contained high amount of chlorine and this was respon-

**Table 2**  
Hardness of the material of construction of the failed bellows.

Location of measurement	Hardness range, HV (100 g load)	
	Inner ply	Outer ply
Root	238–249	215–253
Crest	297–302	273–296

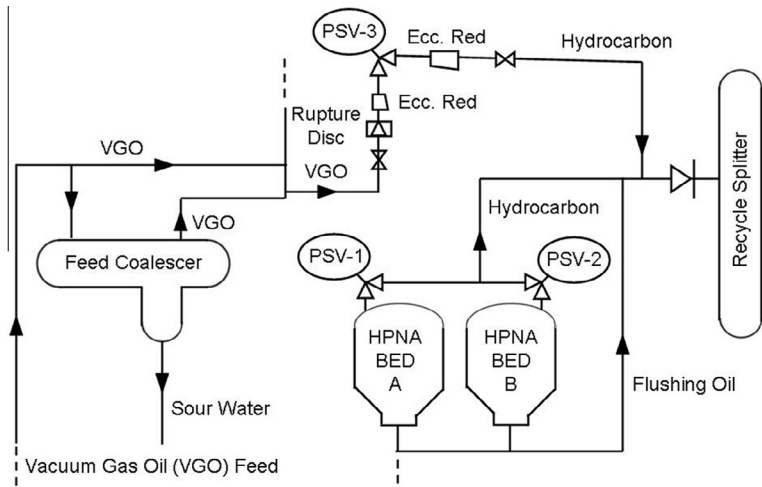


**Fig. 13.** Schematic showing the process flowchart and the associated equipment in the vicinity of failed PSV-3.

sible for the failure of the stainless steel screen by chloride SCC. The HPNA bed was repaired and the hydrocracker unit was re-commissioned. All the three bellows failures occurred after this incident.

Investigation revealed that subsequent to the failure of the bellows, when the PSV was dismantled for repair, its body was found covered with a black deposit. The deposit was formed during the repairing of the HPNA bed and it consisted of activated carbon soot which contained chlorine in high concentration. It was confirmed that this deposit was the source of chloride ions in the system which resulted in a series of bellows failures in the PSV by chloride SCC.



## **1. Introduction**

Hydroprocessing units such as isomax in oil refineries upgrade hydrocarbon feedstocks by converting heavier feeds into more valuable lighter products. The reactions occur under a hydrogen-rich environment at moderately high temperatures and high pressure, in the presence of catalysts. Chemically stabilized austenitic stainless steels such as TP321 and TP347 are widely used for hydro-treater and hydro-cracker in complex refinery, because of their resistance to corrosion resistance and mechanical strength [1–4].

In the present case, investigation has been undertaken after cracks are detected by UT inspection in reactor tube of isomax unit during an overhaul performed after about 210282 h of starting unit.

Reactor tube material is fabricated from AISI 347; this reactor tube with outer diameter 141.3 mm and wall thickness 18.37 mm operates in the maximum temperature and internal pressure of around 522 °C and 190 bar g, both of which are below the design temperature and pressure of 530 °C and 204 bar g respectively.

Probably the biggest cause of failure in pressure plant made of stainless steel is stress corrosion cracking (SCC) This type of corrosion forms deep cracks in the material and is caused by the combined effects of below conditions [4–6]:

- (a) specific environmental conditions with chloride, caustic, high-temperature water, polythionic acids, etc.,
- (b) susceptible material,
- (c) tensile stress.

Stress corrosion cracking by polythionic acids (PTASCC) was first identified with the introduction of hydrotreating units. The first incidence of this phenomenon was reported in 1943 in a fluid catalytic cracker. PTASCC is causes by Ingress of Polythionic acid into the sensitized austenite stainless steel. Polythionic acid is produced due to reaction of air (oxygen) and moisture with the sulfide scale to form polythionic acid [7,8].

According to the refinery operator procedure, after shut down of the furnace for overhaul, first, steam is blown into the furnace tubes to eliminate any residuals. Then, for 7–8 h, steam was blown into the furnace and was vented to air. After that, alkaline washing is used for neutralization. Unfortunately this step just has controlled with duration time and for example, pH changes have not been monitored. Finally, purging with nitrogen or dry air is not performed and the internal surface of tubes is exposed to atmosphere.

During shutdown of hydrocracker unit polythionic acid formation occurred possibly due to errors in shutdown procedures [9].

Austenitic stainless steels and nickel-chromium-iron alloys that have become sensitized through thermal exposure are susceptible to PTASCC.

Sensitization is a deleterious phenomenon that occurs in austenitic stainless steel when it is submitted to an inappropriate increase in temperature such as what happens during welding or operating in the temperature range between 400 °C and 800 °C. This is a well-known phenomenon and consists of carbide precipitation at grain boundaries and chromium depletion in adjacent regions, making the material susceptible to intergranular corrosion [9]. For the AISI 347 the critical temperature is 550 °C that it is very close to design temperature of the reactor heater tubes SS347H [10].

The required tensile stresses can arise from a combination of applied and residual stresses; the later may be caused by weld fabrication or any cold work [11].

Given the above, the above mentioned tube removed and various investigations have been performed to determine the cause of cracks.

## 2. Experimental procedure

In order to determine whether cracks have reached the surface of the tube, dye penetrant test has been performed. According to the RT inspection results, 7 cm from the starting point of RT film, a 3 cm long branched crack has been observed. Therefore Metallographic samples prepared from this section. Samples preparation consisted of grinding down to 2400-grit paper, followed by 1/4 µm diamond polishing. According to ASTM A262 Practice E [12], electrolytic etching was performed in oxalic acid 10%.

Chemical analysis was performed on the cracked tube base material using an AWS PMI MASTER optical emission spectrometer. The interior surface of tube is covered with a black deposit. To identify the presence of sulfur or sulfur based compounds, energy dispersive X-ray spectrographic (EDS) was used. Microstructures of the alloys were observed using optical and scanning electron microscopy. The corrosion deposit in the crack was analyzed using EDS micro-analysis in general accordance with ASTM E1508-98. Microhardness testing (by using Vickers method and 200-gram load accordance with ASTM E 10) was performed on the base metal, HAZ, weld and crack region.

## 3. Results

### 3.1. Dye penetrant inspection

As can be seen in Fig. 1, there are no evidence of cracks on the surface.

After cutting cracked region, the test sample area (Fig. 2) shows the cracks divided to sub branches, which propagated along the weld and the other along the tube direction that has started from the edge of the weld.

### 3.2. Chemical analysis

Results are presented in Table 1. The tube was fabricated from a Type 347 and no unusual conditions were noted.

### 3.3. Microstructural features of the tube material

Fig. 3 shows austenitic microstructure of tube material is away from the weld zone. Chromium carbide precipitation occurs along the austenite grains. This causes depletion of chromium from the austenitic grains resulting in sensitization of material, which weakens the material's ability to withstand certain corrosive environments decreasing the corrosion resistance. Fig. 3 does not show the ditch structure that is representative of a sensitized sample. In the region near the weld as shown in Fig. 4 carbides has precipitated along the grains boundary. Therefore in this region the metal sensitivity was more than the other region.

The crack cross section was prepared for analysis by using an optic microscope. The tip of the crack surface is shown in Fig. 5. The crack surface appears to be intergranular in nature.

Fig. 6 shows the propagation of crack in the tube. The crack propagated on base metal, HAZ and weld.

### 3.4. Deposit analysis

Fig. 7 exhibits the EDS analysis results of deposits that were formed on the surface of the crack.



**Fig. 1.** Reactor tube after dye penetrant test.

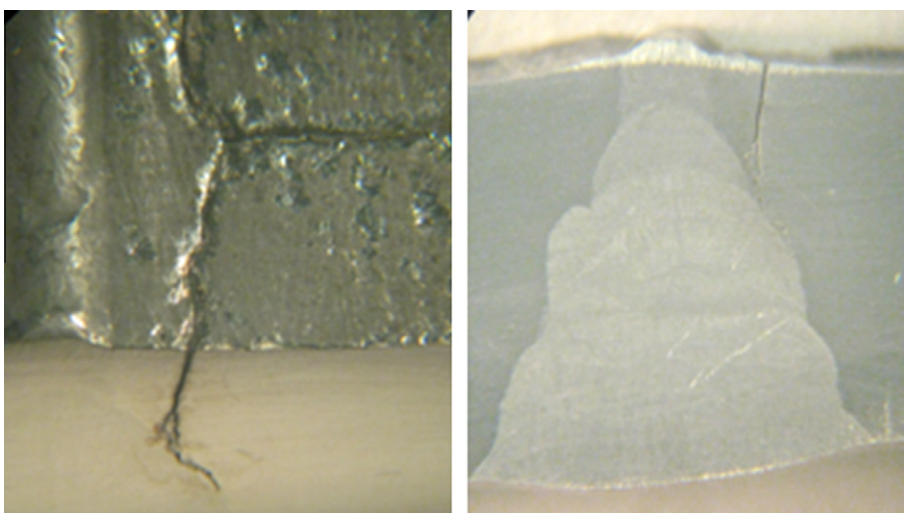


**Fig. 2.** Propagation of branched crack in different weld direction.

**Table 1**

Chemical composition of 347 stainless steel in wt.%

Element specimen	C	Mn	Si	Ni	Cr	Nb	Fe
Heater tube ASTM TP 347 H	0.052 0.04–0.10 max	1.65 2.00 max	0.47 0.75 max	11.7 9.00–13.00	20.1 17.0–20.0	0.62 $8 \times C < Nb < 1.00$	Balance Balance

**Fig. 8** exhibits the EDS analysis results of the crack tip deposits. The results show presence of sulfur (S) in deposits. High percentage of sulfur indicates that the deposit predominantly consists of sulfur components.

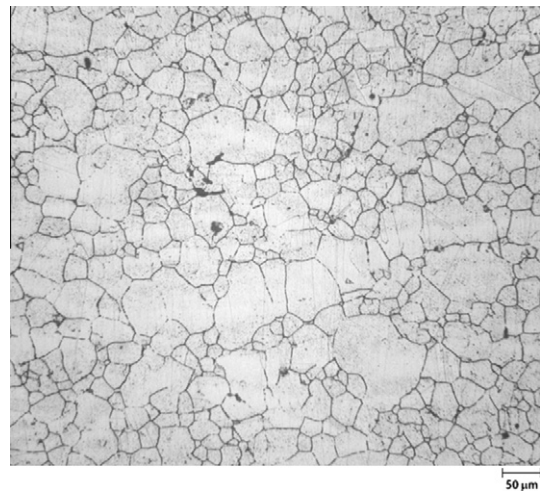


**Fig. 3.** Austenitic microstructure of tube, away from weld zone.

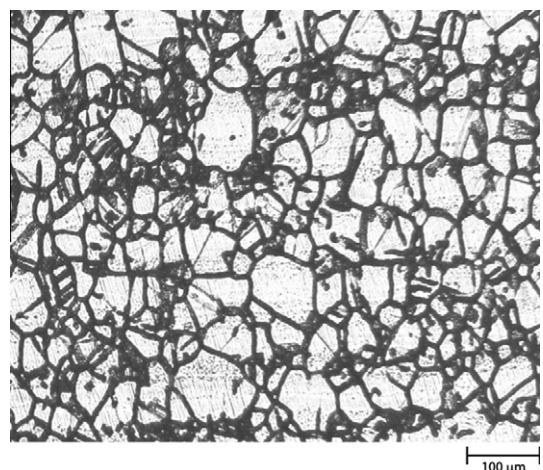


**Fig. 4.** Ditch structure of tube, near weld zone.

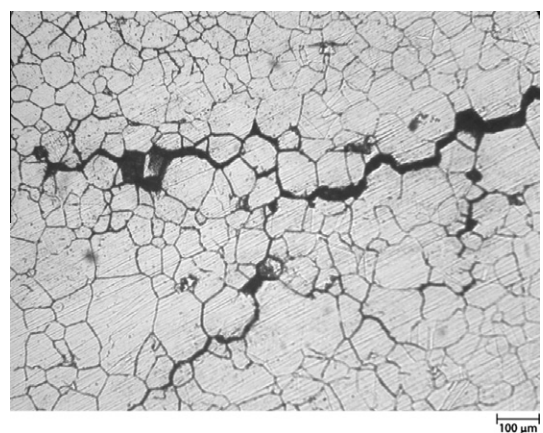


**Fig. 5.** The tip of the crack surface.

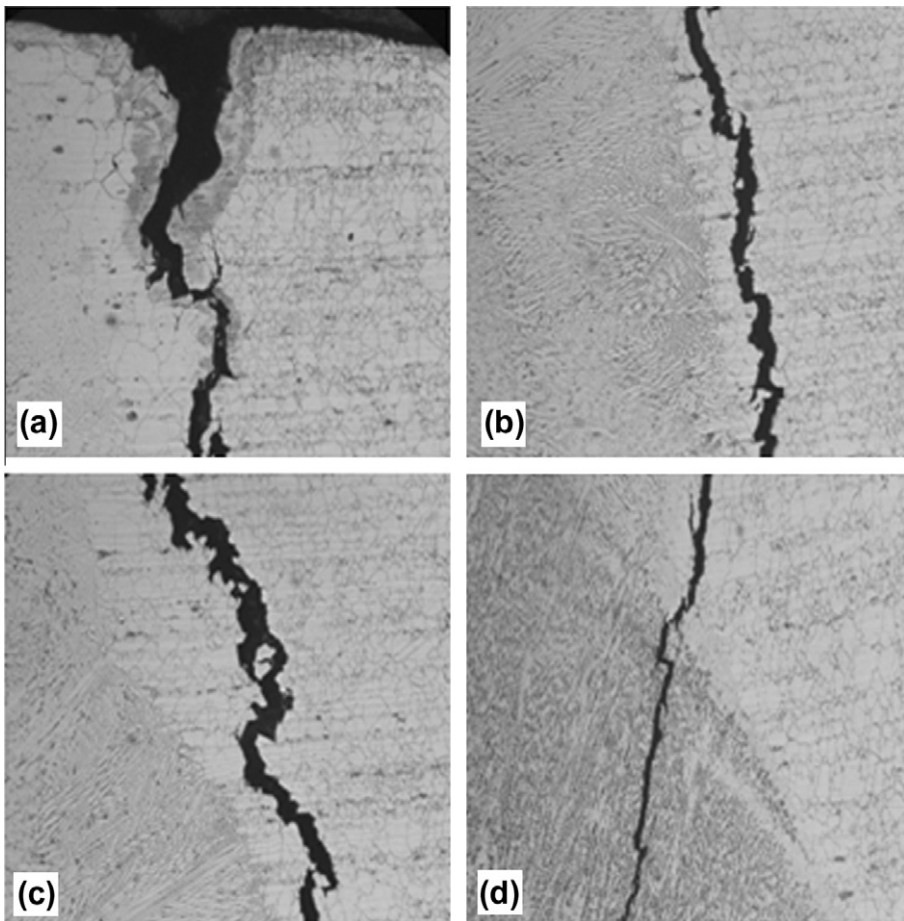


**Fig. 6.** Propagation of crack in tube. (a) Initiation of crack on internal surface. (b) and (c) Propagation of crack in HAZ. (d) Crack propagation in weld.

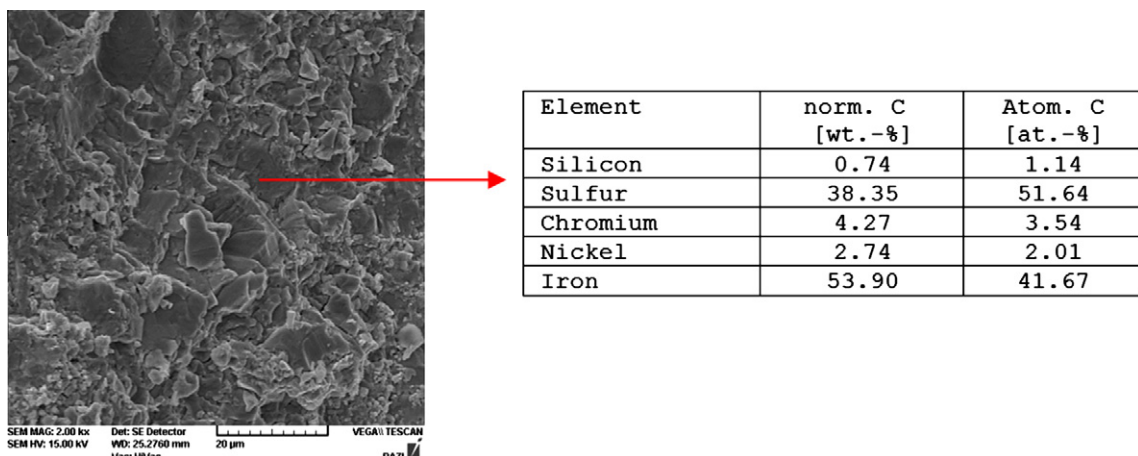
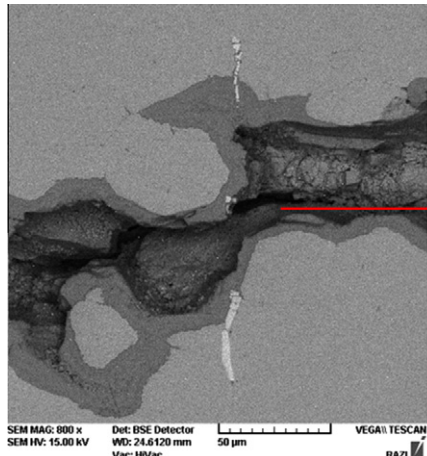


**Fig. 7.** EDS analysis results of the deposits.

### 3.5. PWHT

To investigate effect of PWHT on microstructure of tube alloy, a sample was prepared from it. The sample was divided in two parts. One of them remained intact and another heated to 1065 °C and was kept at this temperature for 10 min. Then the



Element	norm. C [wt.-%]	Atom. C [at.-%]
Oxygen	0.43	1.11
Silicon	1.25	1.84
Sulfur	40.94	52.67
Chromium	35.75	28.36
Manganese	4.11	3.08
Iron	17.52	12.94

Fig. 8. EDS analysis results of the crack tip deposits.

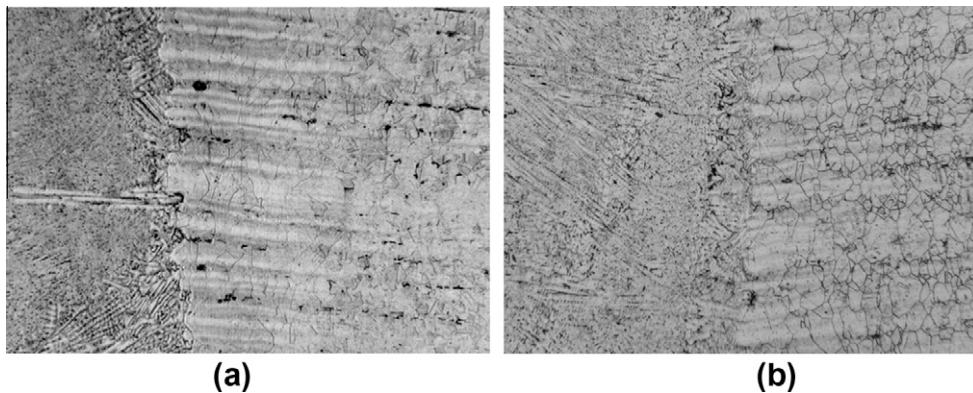


Fig. 9. The microstructure of post weld heat treated sample (a) and the intact one (b).

**Table 2**  
Microhardness testing results (HV).

Region	Base metal	HAZ	Weld	Crack tip
As Received	167	226	244	243
After PWHT	-	154	221	-

temperature reduced to 899 °C. At this temperature, the sample remained for 1 h. Finally, the sample was transferred out of the furnace and air cooled. The microstructure of post weld heat treated sample and the intact one was shown in Fig. 9.

### 3.6. Hardness test

Hardness results are shown in Table 2. As seen, the differences between the hardness of base metal and other regions are significant (approximately 70 Vickers). Furthermore, it can be seen that after PWHT, the hardness of HAZ region has significant decrease.

## 4. Discussion

According the results of analyzing the corrosion deposit, formation of sulfide scales on the inner surface of the reactor tube and in the crack tip were observed, they were formed during operation. During the overhaul, reactor was exposed to

the atmosphere and humidity, sulfide scales react with oxygen and polythionic acid is produced. Also corrosion of grain boundary and presence of sulfur in crack tips that can result in formation of polythionic acid, were observed in EDS analysis.

PTA SCC is a type of intergranular SCC in nature. SCC by polythionic acid is distinguished from other types of SCC due to the intergranular mode of branched cracks propagation which can clearly be observed in Fig. 5.

Another factor of PTA SCC occurrence is tensile stress (residual and applied) that it is usually present in cold equipment and especially associated with weld fabrication [9].

High hardness in welding and heat affected zone (differences between the hardness of base metal and other regions were approximately 70 Vickers) shows that stress relief operation has not been done, that results in presence of residual stress in these areas. According to Fig. 6 the cracking that occurred in a type 347 stainless steel reactor tubes is near the weld and heat affected zone. These cracks are parallel and perpendicular to the weld, reflecting different stress levels in the region.

Metallographical examination indicated that the alloy of reactor tube was sensitized near the weld particularly on heat affected zone.

As it was shown in Fig. 4, due to carbide precipitations at grain boundaries, the observed microstructure of reactor tube alloy is similar to ditch structure and material susceptible to intergranular corrosion, which is another reason for PTA SCC.

Addition of stabilizing elements to alloy, such as titanium or niobium, or limiting the amount of carbon are two methods for reducing the effects of welding and heat treating on sensitization. However, they are not effective in long-term exposure to temperatures above 430 °C. The resistance of stainless steel to polythionic SCC can be significantly improved by a thermal stabilization. Fig. 9 shows the effect of thermal stabilization on microstructure. As can be seen, the microstructure of post weld heat treated sample has changed completely and there are no precipitated carbides in grain boundary. It is clear that, after welding procedure, suitable PWHT has not performed on the evaluated tube. Therefore, PWHT can be done after construction or repair weldings to reduce likelihood of PTA SCC occurrences during the overhaul.

100603611

# Materials safety: article exercise

You are working as a materials expert in your organization and your responsibility is to guarantee safe and efficient use of materials in your facility. One day, a failure in similar facility is brought to your attention, and you need to investigate the possible implications this failure has for your facility. Your job is to interpret and analyze the given failure report and to write a report, which will allow others in your organization to understand the key developments and causes leading to the failure and the necessary actions for prevention of such failures.

Read the given article and analyze the failure. Describe, how the deformation and failure mechanisms presented during the course are reflected in the case and establish the chain of actions leading to the failure. The report should work as an introductory material to your team; it should not be very long but it should enable other team members to understand the key features of the failure without reading the failure report itself.

In addition to establishing the primary cause of the failure, show why alternate failure mechanisms can be ruled out. Some failure mechanisms have not been discussed in the course yet. Conduct the analysis using your present knowledge on the subject.

If the author of the failure analysis has, in your view, neglected to address some aspects of the failure, you may indicate this in your report and suggest tests or actions that should have been done to clarify the issue.

Prepare your response by editing this word document and export it as PDF. The file name identifies you and the article. Do not change the file name (other than the extension to pdf). E-mail the pdf to "materials.safety@iikka.fi".

You may use the question list below to guide you in your analysis:

A. Description of investigation methods applied

- What means of investigation were used in the failure analysis?

Ultrasonic testing (UT) inspection was made to detect the cracks in the reactor tube, during an overhaul, which was made 210282 hours from starting the Isomax hydroprocessing unit.

Dye penetrant testing was made to find out, are the cracks reached the outer surface of the tube.

Radiographic testing (RT) revealed 7cm from the start of the RT film, a branched, 3cm deep crack. From the crack area, metallographic test samples were prepared.

AWS PMI Master optical emission spectrometer was used to perform a chemical inspection to the cracked tube base material.

Energy dispersive X-ray spectrographic was used to identify the presence of sulphur or sulphur-based compounds from the black deposit in the inner wall of the tube.

Optical and scanning electron microscopy was used to observe the microstructures of the alloys. EDS microanalysis was used to analyze the corrosion deposit inside the crack.

Microhardness of the base metal, heat affected zone, weld and crack area was done by using Vickers method and 200-gram load.

- What computational methods were used?

Ultrasonic testing.

Radiographic testing.

Chemical inspection by AWS PMI Master optical emission spectrometer.

Energy dispersive X-ray spectrographic.

Optical and scanning electron microscopy.

EDS microanalysis.

- What material or results were obtained?

Radiographic testing: 7 cm from the starting point of RT film, there was a 3 cm long branched crack.

Interior surface was covered with black deposit.

Dye penetrant testing: No cracks were found from the outer surface.

Cutting the cracked region revealed that the crack propagated in to two branches, from which the other was parallel the weld and other perpendicular to it.

Chemical analysis: showed the tube to be ASTM TP 347 H. There wasn't any unusual conditions noted.

Microstructural analysis: austenitic microstructure was away from the weld. Depletion of chromium from austenitic grains, which causes material sensitization. This decreases material's ability to resist the corrosion. Metal sensitivity was higher near the weld since carbide precipitation was higher in that area.

Optic microscope: crack surface was intergranular in nature. Crack was propagated in weld, heat affected zone and base metal.

EDS analysis of crack tip: deposit consisted mainly of sulphur.

**B. The primary cause of the failure and description of the failure mechanism**

- What is the primary cause of the failure (also provide reasoning)?

Different factors are supporting that the stress corrosion cracking due to polythionic acids (PTA SCC) is the primary cause for the failure.

It was found through the hardness testing that stress relieving process hadn't been done for the weld zone, which had caused residual stresses in that welding area. These stresses are causing SCC to occur.

The tube was made from austenitic stainless steel, which is susceptible for sensitization under high temperatures, which can be caused by welding and in operation temperatures between 400°C and 800°C. Both have altered the failed zone for sensitization due to the welding, in addition to operation temperature of 522°C.

The chromium carbide precipitations occurred along the austenite grains near the weld zone, which through depletion of chromium from austenite grains is decreasing the corrosion resistance and makes it susceptible for intergranular corrosion.

PTA SCC can be separated from other types of SCC with its intergranular nature, and the crack type was intergranular, which is supporting the PTA SCC theory.

The crack was also branched in nature, which is supporting it to be caused by SCC.

Also, sulfide in the crack tip and inner tube wall was found, which can have formed into polythionic acid during the overhaul, when the tube was exposed to atmosphere and humidity. The polythionic acid can also cause corrosion of grain boundaries and presence of sulfur in crack tips, which were found in the EDS analysis.

- What's the chain of action that led to the failure?

When assembling the tube by welding, the area near the welding exposed to high temperature, which assisted the sensitization to occur near the welding area, which decreased the corrosion resistance of that area.

After the welding, stress relieving treatment wasn't done, which left residual stresses near the welding area.

The tube was exposed to temperatures over 400°C, which is also supporting the sensitization to occur in the material.

In the end of the shut-down for doing the overhaul process, the internal surface was exposed to atmosphere and moisture was also possible due to not purging the furnace with dry air. These as a combination is likely to produce polythionic acid together with the sulfide, which was found from the corrosion deposit in the crack tips.

**C. Ruling out alternate failure mechanisms**

- Can plastic deformation be ruled out? If yes, explain how.

There have been residual stresses in the welding area, which can have caused plastic deformation in that area before the cracking. There were also other mechanisms, which supported the PTA SCC, so the plastic deformation is likely to have been smaller than without these other mechanisms, such as the polythionic acid and chromium precipitates. The finer grains among coarse grains are telling also about possible plastic deformation in the area, through recrystallization after elongation of grains.

- Can creep be ruled out? If yes, explain how.

Creep cannot be ruled out, because the material was exposed to high temperatures in its operation and also during welding, in addition to that there was stresses near the welding area affecting to the material at the same time.

- Can brittle fracture be ruled out? If yes, explain how.

Brittle fracture can't be ruled out, because the fracture has been intergranular, which is a sign of embrittlement happened in the material and brittle behavior. The effect of chromium precipitations and polythionic acid can have affected to the embrittlement.

- Can fatigue be ruled out? If yes, explain how.

Fatigue cannot be ruled out totally, if it is assumed that there is variation in the pressure and temperature around the tube during the operation, which can cause changes in stresses during the operation.

- Can environmentally assisted failure be ruled out? If yes, explain how.

Environmentally assisted failure cannot be ruled out because it had important effect on the failure. The tube was exposed to atmosphere and moisture during the shut down procedure, which allowed formation of polythionic acid together with the sulfide, which was found from the corrosion deposit in the crack tips.

**D. Recommendations to prevent similar failures in the future**

The shut down process shall be inspected and plan instructions so, that exposure to humidity and atmosphere is prevented.

The stress relieving process for the welds shall be done, to avoid the residual stresses from occurring in the welding area.

To prevent the sensitization, limiting the amount of carbon, or adding stabilizing elements, like titanium or niobium shall be added to the material.





## 1. Introduction

Owing to a combination of high strength and toughness Fe–Ni–Co–Mo type maraging steels are being used for many critical applications such as aerospace and military [1]. The material is available in different strength ranges and designated as M250, M350, where 'M' stands for maraging steel, 250 and 350 for their yield strength in ksi. Addition of Ni to Fe– system is responsible for thermal hysteresis gap between the formation of martensite on cooling and its reversion to austenite on heating. This hysteresis allowed material scientists to age the material at peak aged condition to achieve optimum properties with moderate level of fracture toughness with martensitic matrix. Increasing the nickel in this system reduces the austenite ( $\gamma$ ) → martensite transformation temperature and it is established that 18% Ni is sufficient to suppress the transformation at RT without rapid cooling from the  $\gamma$ -phase.

Titanium is used as the primary strengthening element and material achieves its strength by precipitation of fine Ti-bearing intermetallic phases dispersed uniformly in the martensitic matrix during aging [2]. Although carbon content is very low, maraging steels are highly alloyed with Nickel, Cobalt, Molybdenum and derive their strength from age hardening of a low carbon, iron, nickel lath martensite. These precipitation hardened Fe–Ni martensitic alloys with very low carbon content meets requirement for fabrication of large sized propellant tanks, bands, tension bolts & studs for space applications [3]. In one such application, maraging steel fasteners (M30X2X90L) were used in nozzle assembly of a satellite launch vehicle.

The fasteners were used in nozzle assembly during one of the static tests and as such they were under sustained load for a period of 2 months under saline humid atmosphere. Further these fasteners were brought in use for some other application, where these fasteners were first given torque to a stress of 180 MPa and were in assembled condition for a period of more than 40 days. When it was further torque to a stress level of 330 MPa, few fasteners sheared off at head-shank junction during torque application. This is to be noted here that these bolts have been used earlier in nozzle assembly during one of the static tests and during that time, they were under sustained load assembly for a period of more than 2 months.

The failed fasteners were subjected to detailed metallurgical investigation to understand the cause for failure. This paper brings out the details of investigation carried out.

## 2. Material

The material used for the fabrication of fasteners was processed through Vacuum Induction Melting (VIM) followed by Vacuum Arc Remelting (VAR). The ingot break down and further hot working was carried out to get rods of 30 mm diameter. The material in solution treated condition ( $820^{\circ}\text{C}$ -1 h-AC) was used for head forming and threads were made through

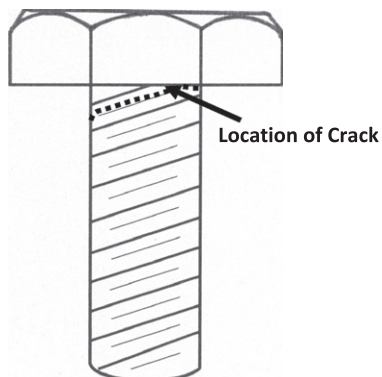


Fig. 1. Schematic of fastener showing location of crack.

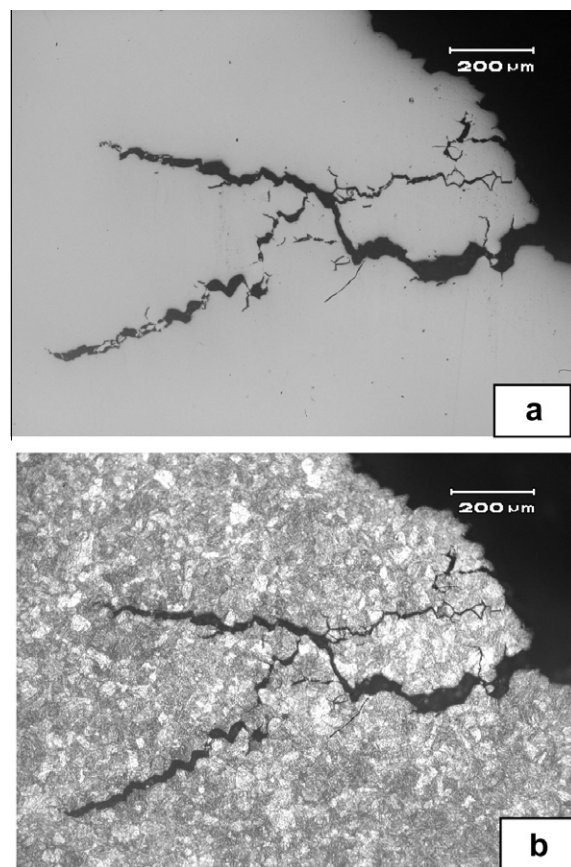


Fig. 2. Optical microphotographs showing secondary cracks from primary fracture edge (a) unetched and (b) etched.

thread rolling. The threaded fasteners were aged to  $480^{\circ}\text{C}$ -3 h-AC to achieve the desired properties. The chemical composition of the alloy in weight percentage was 18.2Ni-4.6Mo-0.42Ti-0.15Al-0.005C-0.02Si-0.022Mn-S&P < 0.005 and balance Fe. Hydrogen was kept low (1 ppm), while oxygen and nitrogen were 15 and 9 ppm respectively. The nominal mechanical properties are YS: min 1725 MPa, UTS: min 1765 MPa, %E on 25 mm, GL: min 8, %RA: min 40 and  $K_{\text{IC}}$ : min 90 MPa $\sqrt{\text{m}}$ .

### 3. Observations

The location of failure in each one of the three failed fasteners was at head-shank junction. Fig. 1 shows the schematic sketch of fastener and location of crack. Evidence of corrosion was seen at and near the fracture edge. Fracture surface had two distinct regions. One all along the periphery had dark and dull, while the region concentric to centre and irregular in shape was bright in appearance. The parts of failed fasteners were cleaned thoroughly using methanol through ultrasonic means. Threaded region near the fracture edge, under optical microscope with stereographic facility revealed a number of cracks at thread root, very near to the fracture edge. The shank portion was cut across its axis and prepared for optical microscopic observations. Fracture path all along the fracture edge was zig-zag and had a number of secondary cracks with branching along grain boundaries, penetrating into the material (Fig. 2). The crack branching resembled feature of tree root morphology. This was further confirmed when specimens were etched with 3%Nital. Features were indicative of anodic dissolution and even at few locations, grains were detached from the matrix. Thread roots nearby fracture edge too had crack initiation at thread root and their penetration with branching (Fig. 3), typical of tree root morphology.

Fracture surface of failed bolt had two distinct regions. Within outer periphery of the fracture surface, multiple secondary cracks penetrating almost perpendicular to the fracture plane were seen (Fig. 4). It was confirmed that crack initiated at and coincided with region of multiple crack at thread root. Fracture surface at the initiation site had predominantly intergranular mode of fracture with presence of secondary cracks (Fig. 5).

The facets on either side of these grain separation had pits resulted due to local preferential corrosion. at certain locations, grain facets had corrosion product left behind crack advancement (Fig. 6). Central part of the fracture surface had predominantly dimple mode of failure (Fig. 7).

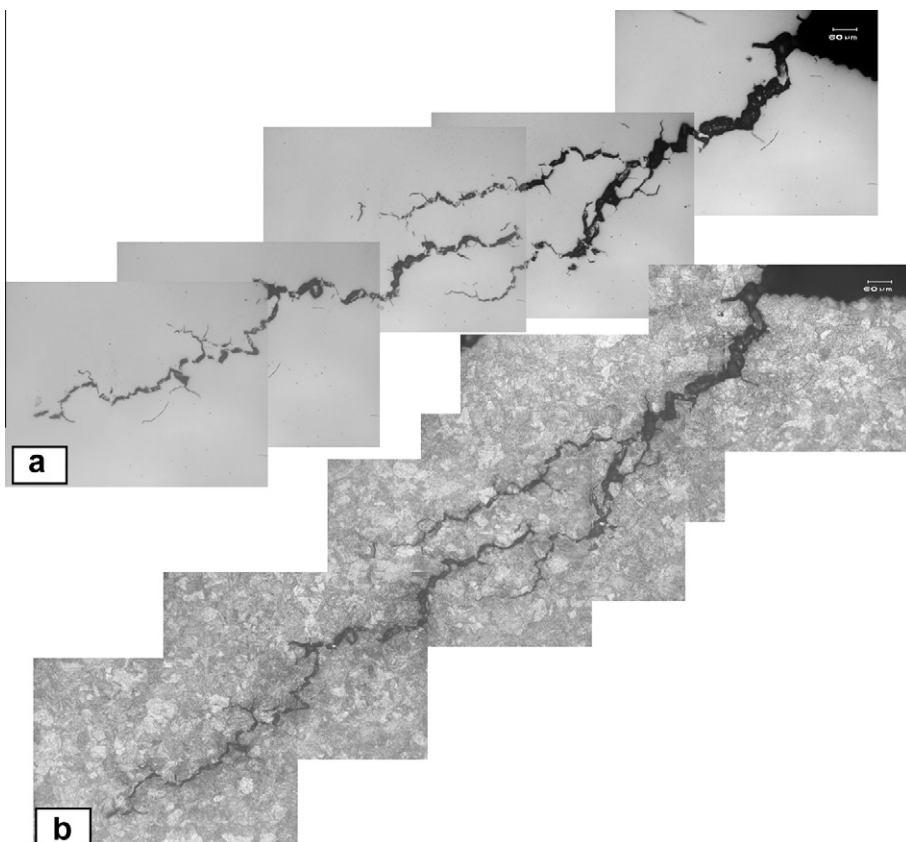


**Fig. 3.** Optical microphotographs showing the crack branching from the thread root near the fracture edge (a) unetched and (b) etched.

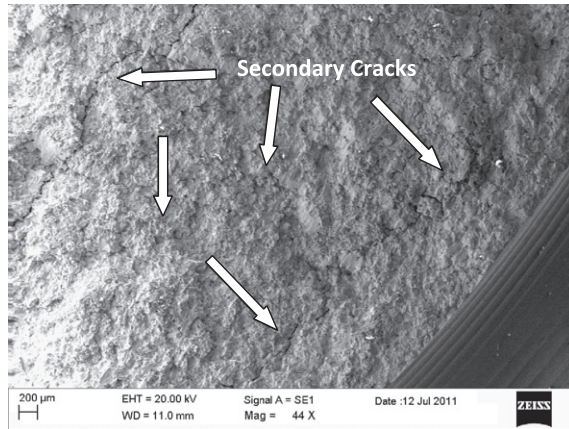


**Fig. 4.** Fractograph showing multiple secondary cracks within outer periphery of the fracture surface.

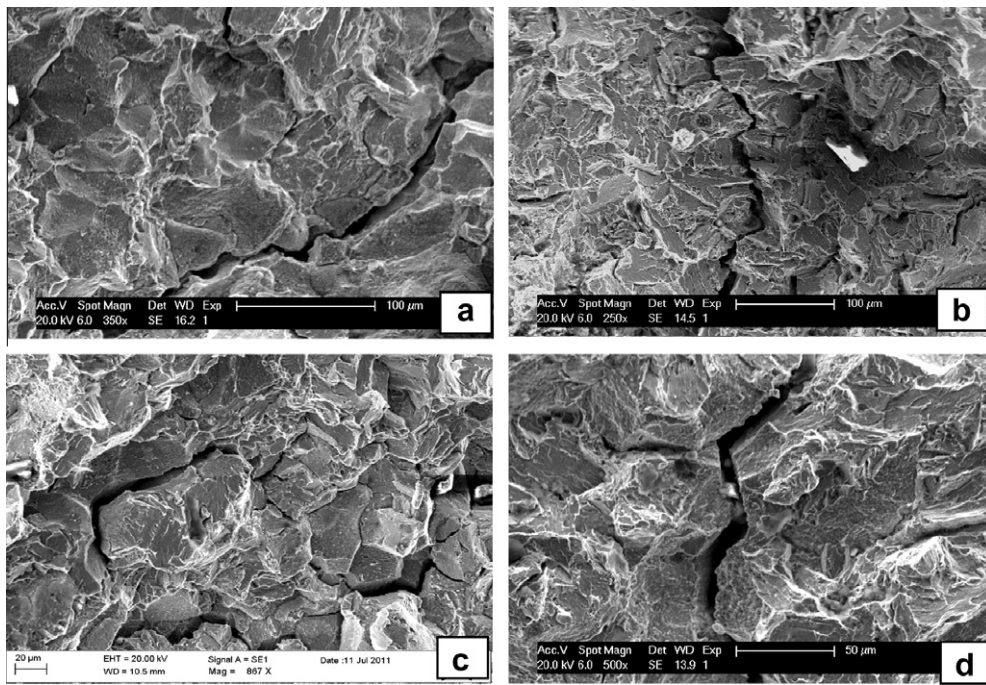


**Fig. 5.** SEM fractographs showing presence of secondary cracks on fracture surface running along the grain boundaries.

#### 4. Discussion

The fasteners were used in nozzle assembly during one of the static tests and as such they were under sustained load for a period of 2 months under humid saline environment. Further these fasteners were used in some other application, where they were in assembled condition under a assembly stress of 180 MPa and when during further torque, stress was raised to 330 MPa, they parted in two. All these indicated this as case of delayed cracking. The intergranular mode of fracture with presence of multiple secondary cracks, evidence of anodic dissolution as evidenced by corrosion product at grain facets indicated failure under synergistic effect of stress (assembly) and corrosion.

It is well established fact that stress corrosion cracking (SCC) resistance of high strength steels in many corrosive media decreases as strength increases. A yield strength of about 1400 MPa and above are vulnerable to catastrophic cracking in corrosive media [4]. The maraging steel grade 18Ni1700 MPa, in solution treated condition with yield strength 1000 MPa showed little or no susceptibility to SCC in 3.5% NaCl solution. The same steel in aged condition with a yield strength of 1700 MPa showed strong susceptibility to SCC [5]. Sastry et al. [6] demonstrated that fracture toughness  $K_Q$  and threshold

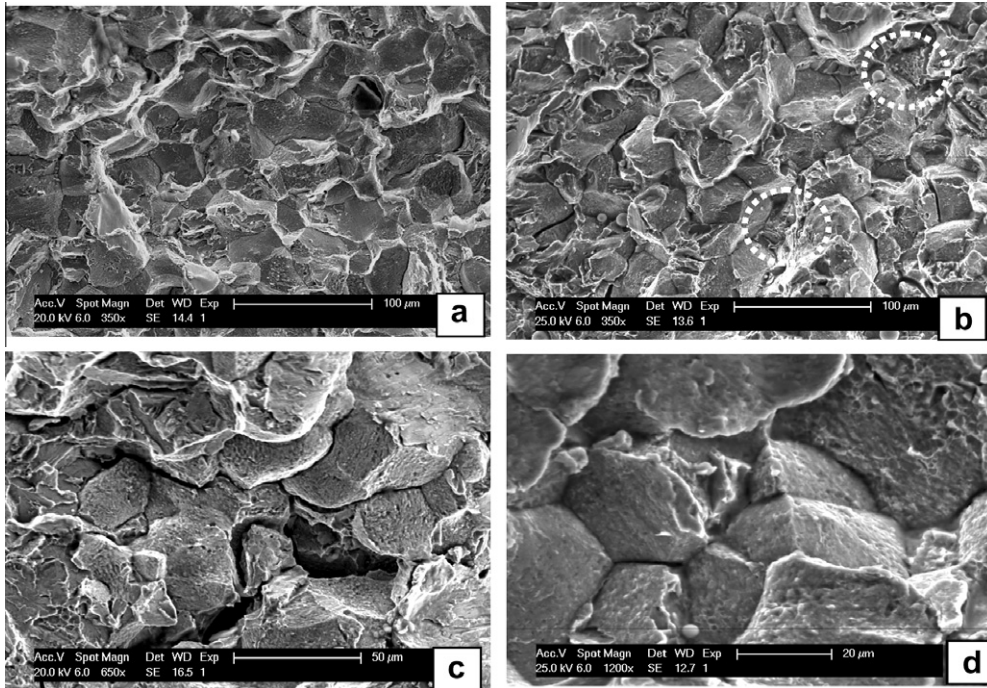


**Fig. 6.** SEM fractographs showing (a) intergranular features, (b) corrosion products and (c and d) pitted facets.

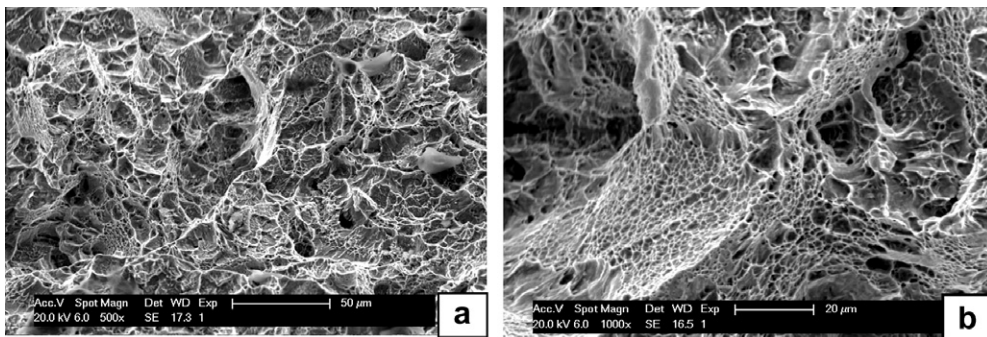


**Fig. 7.** SEM fractographs showing dimple mode of failure within central region of fracture surface.

stress corrosion fracture toughness  $K_{ISCC}$  of the solution treated annealed maraging steel were similar, whereas aging of maraging steel at 480 °C reduced  $K_{ISCC}$  values drastically, as compared to their respective  $K_{ISCC}$  values in an aged condition. The study done by Diwakar et al. [7] indicated that value of critical stress intensity factor  $K_{IC}$  in water came down to the level as low as 8 MPa-m<sup>1/2</sup>. Considering a  $K_{IC}$  value of 10 MPa-m<sup>1/2</sup> for M250 maraging steel, a crack size of even 0.2 mm could not be tolerated for operating stress levels.

The SCC of maraging steel band used for a satellite launch vehicle has been studied by Jha et al. [8], who established that the cracking was intergranular in nature. Stavros and Paxton [9] as well as Rao et al. [10] carried out extensive study on SCC behavior of maraging steel and the crack path was established to be intergranular. Brook and Mucioli [11] also established that the environmental susceptibility was associated with a corrosive susceptible path.

In the present case study, the fastener experienced sustained load and exposed to saline atmosphere of marine coast for a period of 2 months. Further they were in assembly under torque of 50 Kgf-m for 40 days. Cracks at thread roots next to fracture edge and their penetration into the core of material confirmed that simultaneously cracks were active at roots of more than one thread. The corrosion product at crack tip and morphology suggested role of corrosion during crack propagation. Fracture surface had predominantly intergranular mode of fracture, a typical feature of stress corrosion cracking of maraging steel.

Taking considerations of evidences collected from failed fasteners and above discussions, following points converged as conclusive outcome.

1. There was corrosion within the engaged threads, which caused cracks to initiate at thread roots and propagated under influence of load (assembly).
2. Crack propagation was intergranular.
3. Corrosion products at crack tip as well as within grain separation gap were conclusive evidence of anodic dissolution during crack advancement.

887799

# Materials safety: article exercise

You are working as a materials expert in your organization and your responsibility is to guarantee safe and efficient use of materials in your facility. One day, a failure in similar facility is brought to your attention, and you need to investigate the possible implications this failure has for your facility. Your job is to interpret and analyze the given failure report and to write a report, which will allow others in your organization to understand the key developments and causes leading to the failure and the necessary actions for prevention of such failures.

Read the given article and analyze the failure. Describe, how the deformation and failure mechanisms presented during the course are reflected in the case and establish the chain of actions leading to the failure. The report should work as an introductory material to your team; it should not be very long but it should enable other team members to understand the key features of the failure without reading the failure report itself.

In addition to establishing the primary cause of the failure, show why alternate failure mechanisms can be ruled out. Some failure mechanisms have not been discussed in the course yet. Conduct the analysis using your present knowledge on the subject.

If the author of the failure analysis has, in your view, neglected to address some aspects of the failure, you may indicate this in your report and suggest tests or actions that should have been done to clarify the issue.

Prepare your response by editing this word document and export it as PDF. The file name identifies you and the article. Do not change the file name (other than the extension to pdf). E-mail the pdf to "materials.safety@iikka.fi".

You may use the question list below to guide you in your analysis:

- A. Description of investigation methods applied
  - What means of investigation were used in the failure analysis?
  - What computational methods were used?
  - What material or results were obtained?
- B. The primary cause of the failure and description of the failure mechanism
  - What is the primary cause of the failure (also provide reasoning)?
  - What's the chain of action that led to the failure?
- C. Ruling out alternate failure mechanisms
  - Can plastic deformation be ruled out? If yes, explain how.
  - Can creep be ruled out? If yes, explain how.
  - Can brittle fracture be ruled out? If yes, explain how.
  - Can fatigue be ruled out? If yes, explain how.
  - Can environmentally assisted failure be ruled out? If yes, explain how.
- D. Recommendations to prevent similar failures in the future
  - How should the design, material, use, etc. be developed to avoid similar failures in the future? Provide several alternatives and indicate most promising.

**Name: Nguyen Xuan Binh**  
**Student ID: 887799**

## **Materials Safety analysis report on maraging steel fasteners failure**

### **Problem Overview:**

The report investigated the reasons for the failure of maraging steel fasteners used in the nozzle assembly of a satellite launch vehicle. During further torque application, some of these fasteners sheared off at the head-shank junction, indicating a case of delayed cracking. The intergranular fracture, multiple secondary cracks, and anodic dissolution indicates a failure caused by the combined effects of stress and corrosion.

### **A. Description of investigation methods applied**

- What means of investigation were used in the failure analysis?**

From the report, the means of investigation for the failure analysis included:

1. Metallurgical investigation: The failed fasteners underwent a comprehensive metallurgical examination to discern the cause of failure.
2. Vacuum Induction Melting (VIM): metals are melted in a vacuum chamber to prevent contamination from the atmosphere.
3. Vacuum Arc Remelting (VAR): the material is remelted using an electric arc in a vacuum environment. This is a secondary melting process
4. Hot working

- What computational methods were used?**

The author lists a couple of computation methods as follows:

1. Optical microscopy: This method observes the threaded region near the fracture edge. It revealed multiple cracks at the thread root, very close to the fracture edge. Additionally, the shank portion was prepared for optical microscopic observations, which showed the fracture path along the fracture edge with multiple secondary cracks.
2. Scanning electron microscopy fractography: SEM fractography was used to analyze the fracture surface. This revealed features such as intergranular fracture modes, corrosion products, pitted facets, and dimple modes of failure.

- What material or results were obtained?**

**Main result:** The main results obtained are the identifications of corrosion within engaged threads, intergranular crack propagation and evidence of anodic dissolution. This suggests that the material underwent a type of corrosion where the metal acted as an anode, leading to its dissolution and subsequent cracking.

**B. The primary cause of the failure and description of the failure mechanism**

- **What is the primary cause of the failure (also provide reasoning)?**

The primary cause of the failure was the corrosion within the engaged threads of the maraging steel fasteners. This corrosion led to the initiation of cracks at the thread roots.

- **What's the chain of action that led to the failure?**

The chronological order of the fasteners' failure is as follows:

1. Fasteners were initially used in a static test, subjected to a sustained load for 2 months. This exposure occurred in a humid saline environment.
2. Later, in another application, the fasteners experienced increased stress. When torque was applied, raising stress to 330 MPa, some sheared at the head-shank junction.
3. Detailed examination showcased corrosion near the fracture edge. Additionally, multiple cracks were observed at the thread root.
4. The fracture's primary mode was intergranular. This pattern is characteristic of stress corrosion cracking in maraging steel.

**C. Ruling out alternate failure mechanisms**

- Can plastic deformation be ruled out? If yes, explain how.

No, plastic deformation cannot be ruled out. The fasteners were under sustained load in a humid saline environment, which contributed to possible plasticity. When the stress was raised during torque application, the fasteners failed, which can also be a sign of plastic failure.

- Can creep be ruled out? If yes, explain how.

Creep can be ruled out since there is no sign of heavy static loading for an extended time

- Can brittle fracture be ruled out? If yes, explain how.

Brittle fracture cannot be ruled out because the fracture surface had a predominantly intergranular mode of fracture, which is also an indicative sign of creep fracture.

- Can fatigue be ruled out? If yes, explain how.

Fatigue can be ruled out since there is no cyclic loading during analysis.

- Can environmentally assisted failure be ruled out? If yes, explain how.

Environmentally assisted failure cannot be ruled out since this is the main failure mechanism.

**D. Recommendations to prevent similar failures in the future**

- How should the design, material, use, etc. be developed to avoid similar failures in the future? Provide several alternatives and indicate the most promising.

To avoid similar failures in the future, several design, material, and usage recommendations can be inferred from the paper:

1. Protective coatings: Apply corrosion-resistant coatings or treatments to the fasteners. This can act as a barrier, preventing or reducing the rate of corrosion. Surface treatments on the fasteners can offer added protection against environmental factors.
2. Environmental control: If possible, reduce the exposure of the fasteners to corrosive substances. This might involve changing the storage conditions, using seals or gaskets to prevent moisture ingress, or implementing dehumidification systems in areas where the fasteners operate.

572266

## 1 Introduction

This report reviews a failure analysis that was conducted on failed screws in a nozzle assembly. A screw had fractured in half from head-shank junction and along a thread line. The screw was made from 18Ni1700 maraging steel i.e., martensitic and aged steel, and manufactured by hot working an ingot to primary shape, forming a head (at 820 °C – 1 h – AC), and finally rolling threads. The final product was aged at 480 °C – 3 h – AC to achieve desired mechanical properties. The screw was fastened with static stress for two months and in saline humid atmosphere by first applying 180 MPa load for 40 days and after that by increase load to 330 MPa. This is when some of the screws fractured. Nominal yield strength of the 17Ni1700 should be around 1 725 MPa and ultimate tensile strength 1 765 MPa.

## 2 Investigation methods and failure mechanisms

The failed screws were analysed by observing the samples. The sampled were studied by

- macroscopic observations,
- microscopic observations with scanning electron microscope (SEM) and microscope, and
- preparing samples by etching.

The author began the review by observing signs of corrosion around the fracture edge. There are no pictures of the actual fracture surfaces, but the author describes the surfaces by having two distinct regions. The first around the periphery has a dark and dull surface while the more concentric region has irregular shape with bright appearance.

Microscopic analyses were performed to specimen that were prepared by etching. Microscopic observations showed signs of cracks formed at thread root. Cracks are wide and resemble tree root geometry that advanced further within the screw material. Several secondary cracks were found on the fracture surfaces outer periphery that were perpendicular to the fracture plane. SEM photographs show the cracks advancing along grain boundaries and various corrosion products within the grain structure.

## 3 Failure analysis

By combining all evidence from the author's investigation, the most likely primary failure mechanism has been stress corrosion cracking. Conditions to allow stress corrosion cracking have been optimal due to steels susceptibility for corrosion, static tensile load, and humid saline environment. The chain of events that led to the fracture began with assembly and corrosion within thread roots on screw surface that initiated a crack. This crack grew under static load and within corrosive environment. After the crack had grown to critical size, failure occurred as brittle fracture.

There are still other failure mechanisms that should be addressed and possible ruled out as a possibility. Some of them are listed here:

- Plastic deformation can be ruled out as primary failure mechanism. The reported material properties indicate that the screw material is very brittle with high yield strength. The applied stresses are over three times lower than the yield strength of material. There are reported no signs of plastic deformation near fracture surface.

- Creep can be ruled out. The screw has been used in normal operating temperatures that would make failure by creep very unlikely failure mechanism. Grain structure does not show signs that would directly indicate failure by creep, such as voids between grain boundaries.
- Brittle fracture can be ruled out as primary failure mechanism. Brittle fracture has most likely occurred after main crack has reached its critical size.
- Fatigue can be ruled out as primary failure mechanism. Fatigue would require a cyclic load to occur and the screw has been under static load.

For future recommendations, either part design or material selection should be reviewed. the screw threads should be protected from corrosive environment. This could be done by sealing the threads or sealing the surface under screws head. Other option would be to select other material that is not susceptible to stress corrosion cracking.